International Journal of Thin Films Science and Technology

http://dx.doi.org/10.18576/ijtfst/130307

# Optimization of Thickness, Energy Band Gap, and Temperature for High Efficiency of Lead Halide Perovskite Solar Cell

*Hussein. A. Rshash*[1,*] *and Samer M. Abdul Almohsin*[1,*].

[1] Department of Physics, College of Education for Pure Science, Thi Qar University, Thi-Qar,64001, Iraq.

Received: 7. Jun.2024, Revised: 11.Aug. 2024, Accepted: 25 Aug. 2024
Published online: 1 Sep. 2024

**Abstract:** In this paper we investigate the inorganic hole and electron transport layer of FTO/$TiO_2$/CH3$NH_3PbI_3$/CuI/Ni structure solar cells through the SCAPS-1D software program. It consists of the absorber layer $CH_3NH_3PbI_3$, electron transport material $TiO_2$, and hole transport material which is CuI in addition to front and back electrodes FTO, and Ni, respectively. The study included the effect of several factors such as changes in thickness and band gap for the active layer, ETM, HTL., and thickness for back electrode Ni on the efficiency of the solar cell. All studies were under a constant temperature of 300k. Finally, the efficiency of the proposed cell was tested under a range of different temperatures. We found the optimum values of photovoltaic parameters including, Fill factor (FF), Short circuit current density ($J_{sc}$), Open circuit voltage ($V_{oc}$), and power conversion efficacy (η) for solar cells. The efficiency of the proposed solar cell is 20.63% and $V_{oc}$ = 2.012 V, Jsc = 26.653 mA/cm$^2$, and FF= 38.33%.

**Keywords:** lead halide, perovskite, $TiO_2$, CuI, Solar cell.

## 1 Introduction

One of the most significant renewable and green energy sources, solar energy is also a significant source of renewable and environmentally friendly energy. It provides energy solutions for sustainable development. Applications for concentrated solar power and solar photovoltaics are always being developed to suit our energy needs. [1]. Perovskite solar cells (PSCs) are the most promising technology to be commercially available in the market among the third generation of photovoltaic (PVs) for their distinctive properties. Significant improvements in efficiency and stability have been observed in lab environments [2][3]. The perovskite layer is sandwiched between electrodes , commonly used as an oxide Transparent that conducts charge carriers (FTO) and a Metal, and two charge transportation layers [ETL] and [HTL][4][5].

There have been instances of a wide range of organic-inorganic hybrid metal iodide perovskites with the general formula AMI3, where A is the methylammonium (CH3NH3+) or formamidinium (HC(NH2)2+) cation. and M is tin (1 and 2) or lead (3 and 4) are reported. Based on optical absorption tests, 1-4 shows the properties of direct-gap semiconductors, with energy band gaps dispersed between 1.25 and 1.75 eV. At room temperature, the compounds show an intense near-IR photoluminescence activity in the 700–1000 nm region (1.1–1.7 eV)[6][7]. One M metal cation that has been employed is lead (Pb). However, because lead is hazardous it's prevented from being available commercially [8]. shown that while tin may substitute lead, it reduces the solar cell's performance conversion efficiency[9].$CH_3NH_3PbI_3$ becomes a superb light harvester because of its outstanding characteristics, which include a variable band gap, long diffusion length, perfect band gap, broad absorption spectrum, and good carrier transport mechanisms. It is also easy to produce on a flexible substrate. The lead halide perovskite has high qualities making it promising to employ in the creation of perovskite solar cells and increasingly an effective substitute for the conventional silicon material[10].

Titanium oxide has been acknowledged as a fundamental ETL in PSCs over the past decade because of its low processing temperature, improved stability, and appropriate optoelectronic properties. shown to be the best [ETM] ,with a 4.1 eV [CBM], Its [VBM] is at a very low location, and its CBM is marginally lower than that of CH3NH3PbI3, ensuring electron injection from perovskite absorber to ETL by direct contact[11][12]. TiO2 is a significant semiconductor that has drawn interest in photochemical synthesis solar cells. It is inexpensive, non-toxic, and environmentally friendly. With extremely distinctive chemical, physical, and material features, it is one of the most plentiful materials on Earth. Its exceptional optical transmittance in the visible and near-infrared wavelengths, high dielectric constant, and photocatalytic activity are only a few of its special qualities. Its 3.2 eV band gap is rather wide. Its large energy band gap makes it a useful material in the ultraviolet. TiO2 is an extremely intriguing substance for many areas of scientific study, industrial use, renewable energy, and environmental protection because of these unique features[13][14][15].

*Corresponding author E-mail: hussinali.phsx@utq.edu.iq

CuCl, CuBr, and CuI are copper halides that are of special importance because of their competitive characteristics when compared to II-VI and III-nitrides. Large direct band gaps [for CuCl = 3.3 eV, CuBr =2.91 eV f, and CuI =2.95 eV-3.1 eV], a significant temperature dependency. and height exciton binding energies {190 meV for CuCl, 108 meV for CuBr, and 63 meV for CuI}. Because of their large range of densities of holes ($10^{16}$ - $10^{20}$ $cm^3$), transparent copper(I) halides, such as CuI, have significant hole mobility equal to [44 $\frac{Cm^2}{V.S}$]. P-type conduction which arrive 280 $\frac{S}{cm}$ [16]. When compared to Cu(I)-based oxides, CuI exhibits superior electrical performance for two reasons: (A) the electronegativity of iodine is smaller than that of oxygen [2.66 against 3.44 on the Pauling scale], allowing for more delocalized holes above the VBM. and (B) the large I− radius of 220 pm and the spatially spread three outermost p-orbitals can achieve sufficient orbital overlap for fast hole transport[17]. and organic-lead-halide perovskite solar cells, which primarily owe their exceptional performance to CuI 's high hole mobility. Recently, studies on CuI thin films as a transparent p-type semiconductor for transparent electronics applications have also been started[18][19]. Due to CuI's many special qualities, including its high hole mobility, low cost of manufacture, ease of deposition, and superior chemical stability[20].

As a result, it is suitable for highly efficient perovskite solar cells. The $CH_3NH_3pbI_3$-based PSCs FTO/PCBM/CH3NH3PbI3/PEDOT: PSS/Ag was done using a Solar Cell Capacity Simulator (SCAPS). the results as follows; PCE= 31.77%, $J_{sc}$ = 25.60 mA/$cm^2$ ,$V_{oc}$= 1.52V, FF= 81.58% [10]. In a different simulation-based investigation (SCAPS), TiO2 and CuI were utilized. Within the solar cell model Glass/TiO2/ZnO: Al/CH3NH3SnI 3/CuI/Au. It showed the following results PCE= 25.91%,$J_{sc}$= 31.77mA/$cm^2$,Voc = 1.04V,FF= 78.18% [21]. Using a simulation(SCAPS) the model TCO/$MoS_2$/$CH_3NH_3PbI_3$/$TiO_2$/Ag showed the following results PCE= 20.43%,$J_{sc}$= 26.24mA/$cm^2$,Voc = 0.93V,FF= 83% [22].

These Manuscripts suggested the optimum structure FTO/$TiO_2$/$CH_3NH_3pbI_3$/CuI/Ni. The projected consumes are designed and inspected by the simulation software program SCAPS-1D. At the University of Gent at Belgium's Department of Electronics and Information Systems. to simulate solar cells, the Solar Cell Capacitance Simulator One-Dimensional program was created. For the free electrons and holes in the conduction and valence bands, Poisson's equation and the continuity equation are included, numerical simulations can be credited to its single blend of accuracy, versatility, operative sociability, open-source nature, and the active provision from its communal of users and developers[23].

So, we current the SCAPS-1D examine numerical modeling of the inorganic hole and electron transport layer of FTO/$TiO_2$/CH3$NH_3PbI_3$/CuI/Ni. Usually, the effect changes the thickness and band gap for both the active, electron and hole transport layer. In addition to the effect of temperature on the solar cell's fundamental parameters. Our modelled outcome will be a step forward should be investigation the ideal conditions for achieving high efficiency solar cells.

## 2 Materials and methods

**2.1 Solar cell structure**. Figure 1 shows a schematic representation of the solar cell structure that was employed in the simulation. Normally, N-$TiO_2$ was used as ETM, P-CuI was employed as the hole transport layer (HTL), while i-$CH_3NH_3pbI_3$ was used as the active layer for our configuration n–i–p solar - cells. Transparent conductive oxide [FTO] and Nickel [Ni] Used as metal electrodes (front and back) of the device.

### 2.2 Numerical simulation and parameters of materials

In our present research, SCAPS-1D software is a powerful and valuable numerical simulation tool to recognize and clarify the physical phenomena arising in photovoltaic devices[24]. The numerical simulation software called SCAPS-1D was developed by researchers from the University of Gent's Electronics and Information Systems (ELIS) Department. It makes use of the Poisson equation and the continuity equation for electrons and holes in steady-state conditions. Free electrons and holes in the conduction and valence bands are treated using Poisson's and continuity equations.[25]. allows up to seven heterojunction layers to be designed and simulated. The following are the continuity equations for electrons and holes[26][23]:

$$-\left(\frac{1}{q}\right)\frac{d_{jn}}{dx} - U_n + G = \frac{d_n}{dt} \quad (1)$$

$$-\left(\frac{1}{q}\right)\frac{d_{jp}}{dx} - U_p + G = \frac{d_p}{dt} \quad (2)$$

where G is the generation rate, $J_n$ and $J_p$ are the current densities for electrons and holes, respectively. The Poisson formula is as follows:

$$\frac{d^2}{dx^2}\psi(x) = \frac{e}{\epsilon_o\epsilon_r}\left(\rho(x) - n(x) + N_D - N_A + \rho_p - \rho_n\right) \quad (3)$$

where e is the electrical charge, $\varepsilon_r$ is the relative, $\varepsilon_0$ is the vacuum permittivity, ψ is the electrostatic potential, p and n are the concentrations of holes and electrons, respectively, $N_A$ and $N_D$ are the charge impurities of the acceptor and donor types, respectively, and $\rho_p$ and $\rho_n$ are the distributions of holes and electrons, respectively. In this research succeeding the standard test conditions (STC), the spectrum used in all simulations was the AM1.5G spectrum, the incident light power was set at 1000 W/m2, and the temperature was set at 300 K. The parameters of CuI, $CH_3NH_3pbI_3$, $TiO_2$, FTO utilized to carry out our numerical

simulations are listed in Table 1 based on References.[27][21][28][29][30][31].

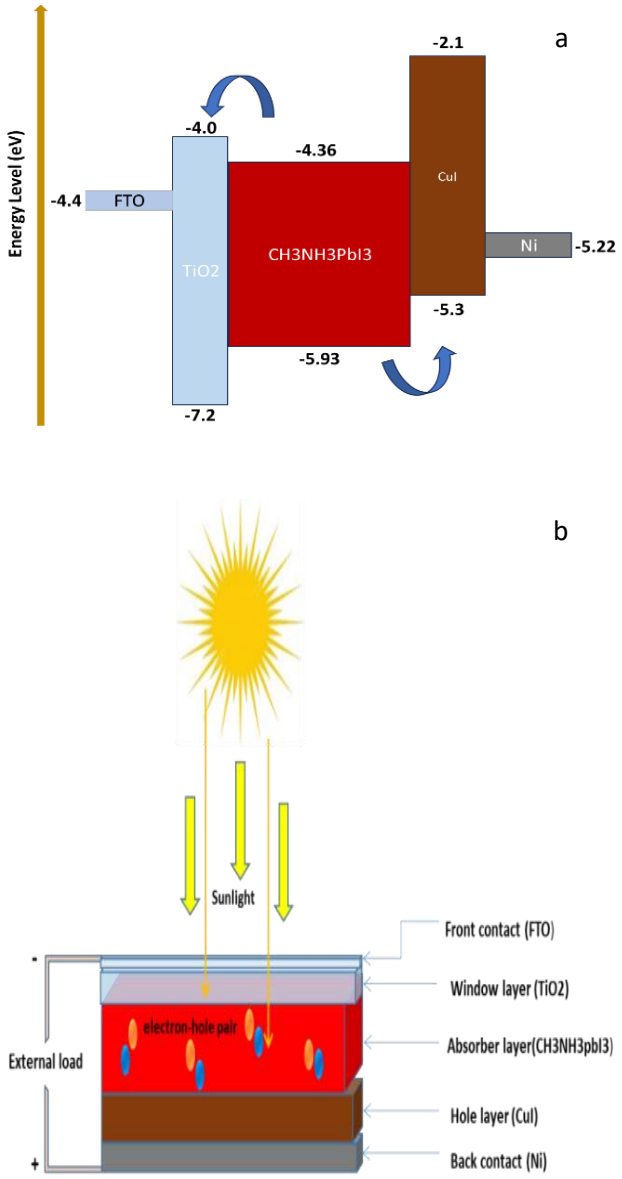


**Scheme 1:** Schematic illustration of simulated devices. (a) The basic schematic diagram of the FTO/$TiO_2$/$CH_3NH_3pbI_3$/CuI/Ni perovskite solar cell device structure. (b) energy band diagram of materials used.

**Table 1:** The initial parameters employed in our simulations of FTO/$TiO_2$/$CH_3NH_3pbI_3$/CuI/Ni.

| Material parameter | FTO | TiO2 | $CH_3NH_3pbI_3$ | CuI |
|---|---|---|---|---|
| Thickness(µm) | 0.25 | 0.05 | 3 | 0.1 |
| Band gap, Eg (eV) | 3.5 | 3.2 | 1.55 | 2.98 |
| Electron affinity, χ (eV) | 4 | 4.26 | 3.9 | 2.1 |
| Permittivity (Relative), $\varepsilon_r$ | 9 | 50 | 10 | 6.5 |
| CB density of states ($cm^{-3}$) | $2\times10^{+18}$ | $1\times10^{+21}$ | $2.78\times10^{+18}$ | $1\times10^{+19}$ |
| VB density of states ($cm^{-3}$) | $1.8\times10^{+19}$ | $1\times10^{+20}$ | $3.9\times10^{+18}$ | $1\times10^{+19}$ |
| Mobility (Electron), µn ($cm^2$/Vs) | 20 | $6\times10^{-3}$ | 10 | $1.69\times10^{-4}$ |
| Mobility (Hole), µh (cm2 /Vs) | 8 | $6\times10^{-3}$ | 10 | $1.69\times10^{-4}$ |
| Acceptor density ($cm^{-3}$) | 0 | 0 | 0 | $1\times10^{+18}$ |
| Donor density ($cm^{-3}$) | $2\times10^{+19}$ | $5\times10^{+19}$ | $1\times10^{+19}$ | 0 |
| Defect density ($cm^{-3}$) | 0 | 0 | $1\times10^{+14}$ | 0 |

## 3 Results and Discussion

### 3.1 Impact of changing thickness, Band Gap for HTL

Figure [1,2] shows the impact of the thickness hole layer and band gap on solar- cell performance metrics, such as, short circuit current density ($J_{SC}$), open circuit voltage ($V_{OC}$), fill factor (FF), and power conversion efficiency (PCE).

In this study, we changed the CuI layer's thickness from 0.1µm to 1µm as shown in Figure 1(a) most of the photovoltaic parameters had a drop on the change in thickness of the CuI layer. The $V_{oc}$ decreased from about 1.35 V at a thickness of 0.1 µm to about 0.97 eV at a thickness of 1µm. while the $J_{sc}$ values are nearly constant for every CuI thickness which varied from 0.1 toward 1µm. While varying the hole thickness from 0.1 µm to 1 µm, the FF increases from 55.52% to 70.40% then it drops to 70.21% at 1µm, and efficiency decreases from 16.21% to 14.79%.

These results could be explained as the thickness increases, Additionally, the decrease in [PCE] with increasing thickness is connected with the speeding up of electron-hole pair recombination due to an increase in the path for the hole that reduces the probability of passing it through the thicker layers. This causes an increase in series resistance causing a reduction in $V_{oc}$ and $J_{sc}$[26]. As a result, the full factor increases, while the efficiency decreases according to the following equations[28]:

$$FF = \frac{J_{max} \cdot V_{max}}{J_{sc} \cdot V_{oc}} \quad (4)$$

$$\eta = \frac{J_{SC} \times V_{OC} \times FF}{P_{in}} \quad (5)$$

Thereby, the thickness of HTL(CuI) is taken to be 0.1µm for the optimized solar cell structure.

Figure 2 shows the variations of the solar cell output parameters $V_{oc}$, $J_{sc}$, FF, and η. energy band gap for CuI. Here, the energy band gap varies from 2.95eV to 3.03eV. the $V_{oc}$ increases dramatically from 1.48 V to 7.62 V. Almost constant Jsc values can be observed for every CuI energy band gap which is 24.69 mA/$cm^2$. the FF decreased from 51.14% to 10.43%. the PCE(η) increases significantly from 18.73% to 19.64%. Through the study, it was found the band gap for CuI wide. It's well-suited for effective hole transport. The valence band of CuI is energetically aligned with the valence band of the perovskite, facilitating efficient hole transfer from the perovskite to the CuI HTL. This alignment minimizes energy loss during hole transport, improving the overall efficiency of the solar cell. Therefore, an HTL(CuI) energy band gap of 3.03eV is considered to be the optimal solar cell structure.

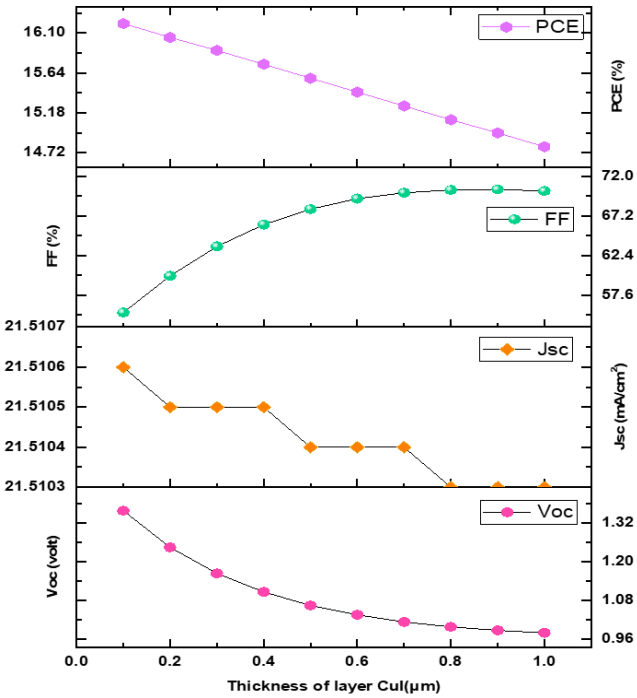


**Fig. 1:** The variation of $V_{oc}$(v), $J_{sc}$(mA.cm$^{-2}$), FF (%), PCE(η) (%) with thickness layer of CuI in(µm).

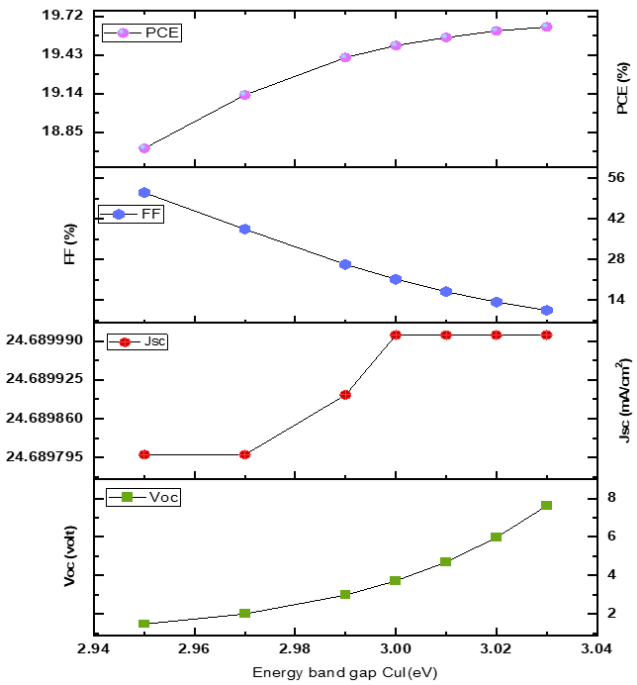


**Fig. 2:** The variation of Voc(v), Jsc(mA/cm$^2$), FF (%), PCE(η) (%) with energy band gap for CuI.

### 3.2 Study Thickness and Band gap of the active layer

Figure [3,4] provides a depiction of the influence of the thickness absorber layer and band gap on solar cell output performance.

We increase the thickness as shown in the fig.3 which varies from 0.25 µm to 3 µm. Here, the $V_{oc}$ decreases from 4.05V at 0.25µm to 1.35V at 3µm. As for $J_{sc}$ increases from 18.85 mA/cm$^2$ at 0.25µm to 24.68 mA/cm$^2$ at 1µm then decreases to 21.51 mA/cm$^2$ at 3µm. the FF increases significantly from 19.47% at 0.25 µm to 55.52% at 3µm. While PCE(η) rise from 14.89% at 0.25µm to19.03% at 1µm then drop to 16.21% at 3µm. This may be because when electron-hole pairs are created in a solar cell's absorber layer upon light incident. The solar cell must function properly so that these pairings reach every electrode without recombining. In cases when the perovskite absorber layer thickness is overly thick ,it lengthens the time needed for light energy to be absorbed and converted, which causes recombination, which would lower the current density (Jsc), and voltage (Voc). which leads to increased FF and decreased PCE according to the equations (4,5). On the other hand, a perovskite absorber layer that is too thin may prevent light from being absorbed.[26]

Figure 4 shows the solar cell output parameters $V_{oc}$, $J_{sc}$, FF, and η with variations of energy band gap for $CH_3NH_3pbI_3$. Here, the energy band gap varies from 1.25eV to 1.55eV. the $V_{oc}$ increases dramatically from 0.82V to 7.62V. The Jsc values decrease with the change energy band gap from 34.16mA/cm$^2$ to 24.69mA/cm$^2$. the FF values increase from 50.93% to 75.61% at 1.4eV then it decreases to 10.43% at 1.55eV. the PCE(η) increases significantly from 14.38% to 20.38% then it decreases to 19.64% at 1.55eV. The local collection efficiency of light absorption as the energy band gap rises, quickening the rate of carrier creation and rises the Voc according to the equation[23]:

$$V_{oc} = \frac{K_B T}{q} \ln\left(1 + \frac{I_{ph}}{I_0}\right) \quad (6)$$

In this work, the thickness and energy band- gap of the absorber- layer were chosen at 1 µm and 1.5 eV, respectively, which are the ideal values for the proposed solar cell.

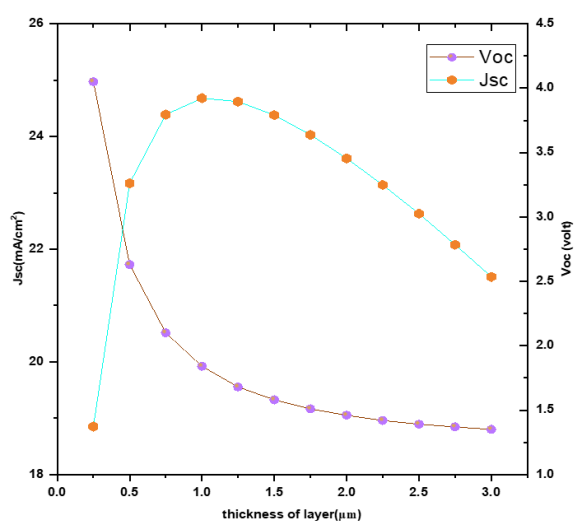

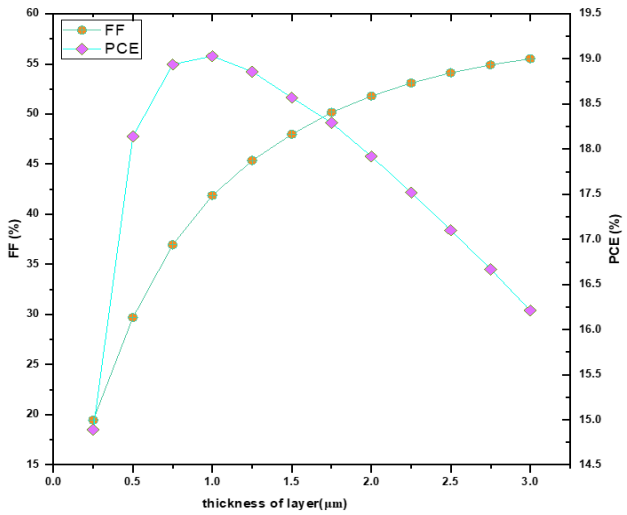


**Fig. 3:** Impact of absorber layer [$CH_3NH_3pbI_3$] thickness on $V_{oc}$(volt), $J_{sc}$(mA/cm$^2$), FF (%), and PCE (%). (a) Impact of absorber layer $CH_3NH_3pbI_3$ thickness on $V_{oc}$(volt) and $J_{sc}$(mA/cm$^2$). (b) Impact of absorber layer $CH_3NH_3pbI_3$ thickness on FF (%) and PCE (%).

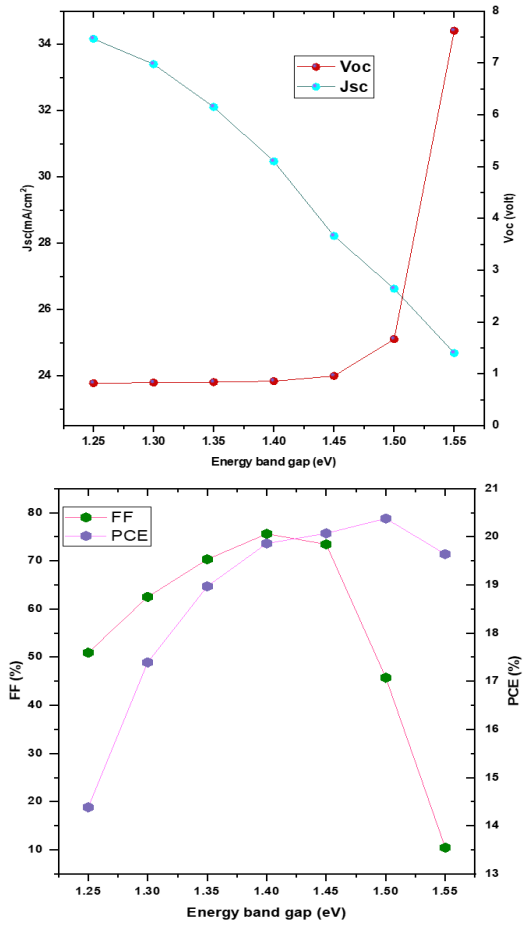


**Fig. 4:** Impact of absorber layer [$CH_3NH_3pbI_3$] energy band gap on $V_{oc}$(volt), $J_{sc}$(mA/cm$^2$), FF (%), and PCE (%). (a) Impact of absorber layer $CH_3NH_3pbI_3$ energy band gap on Voc(volt) and Jsc(mA/cm$^2$). (b) Impact of absorber layer $CH_3NH_3pbI_3$ energy band gap on FF (%) and PCE (%).

### 3.3 Effect of ETM ($TiO_2$) Thickness and Band gap.

Figure [5,6] shows the variation of photovoltaic parameters concerning the ETL thickness and its energy band gap.

$TiO_2$ is used as the first material to be exposed to incoming light in the n-i-p structure as an [ETL] material. $TiO_2$ thickness optimization is crucial for the initial device manufacturing. Consequently, the impact of altering the layer thickness from 0.01 toward 1 μm on the parameter of the solar cell was studied. As shown in Fig. (5), the PCE(η) values remain constant for each $TiO_2$ thickness, while the Voc, Jsc, and FF values change slightly. These results can be explained by the nature of $TiO_2$ which has high mobility and fewer defects therefore the electron is not affected much by increasing the thickness of $TiO_2$.

The band gap of the ETL is essential for creating solar cells with high efficiency. The effect of the ETL band gap on solar output characteristics is depicted in Figure (6). The $TiO_2$ band gap in the ETL changes from 2.96 eV to 3.3 eV. When the energy band gap of the ETL changes fro-m 2.96 eV to 3.3 eV, we find that PCE (η) 20.38%, FF 45.73%, Jsc 26.633 mA/cm2, and Voc 1.673 V are almost constant due to the small change in energy gap does not affect the configuration alignment of solar cells.

The ETL optimal thickness and energy band gap for the suggested solar cell are 0.05μm and 3eV, respectively, which were selected in this study.

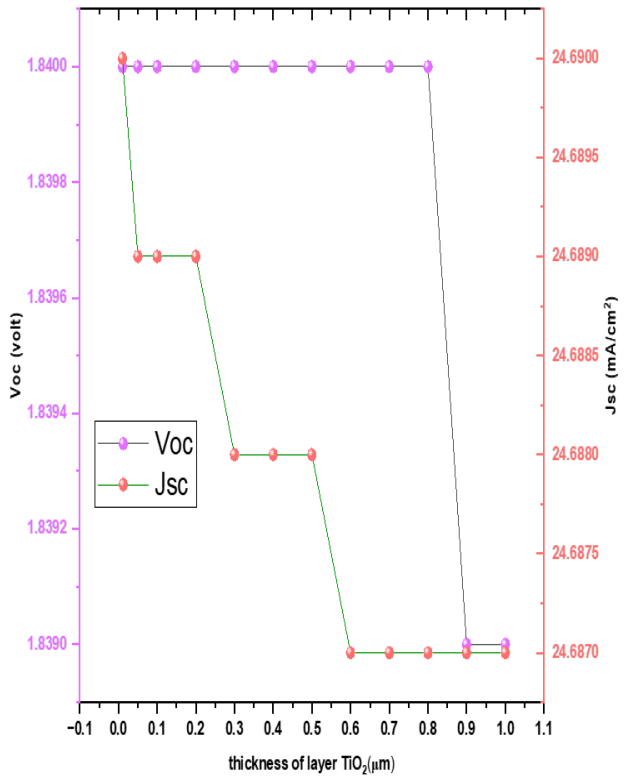

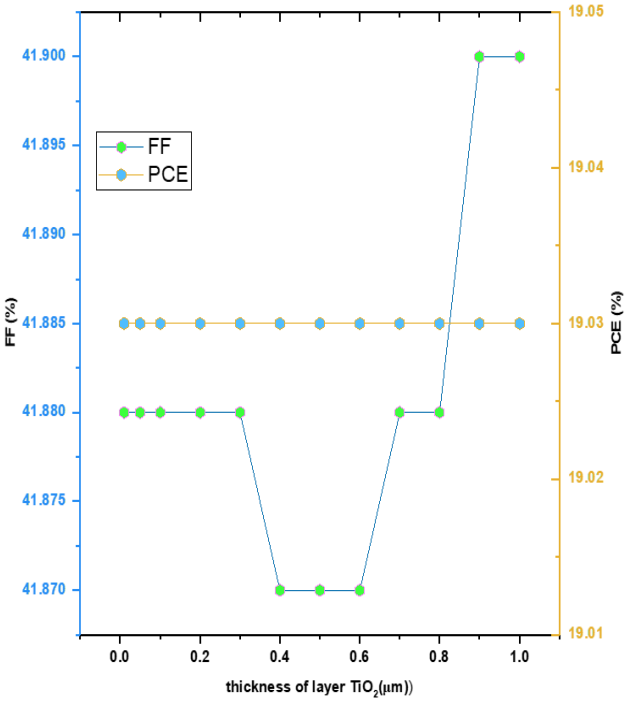


Fig. 5: Impact of ETL [$TiO_2$] thickn-ess on $V_{oc}$(volt), $J_{sc}$(mA/cm$^2$), FF (%), and PCE (%). (a) Impact -of ETL $TiO_2$ thickness on Voc(volt) and Jsc(mA/cm$^2$). (b) Impact of ETL $TiO_2$ thickness on FF (%) and PCE (%).

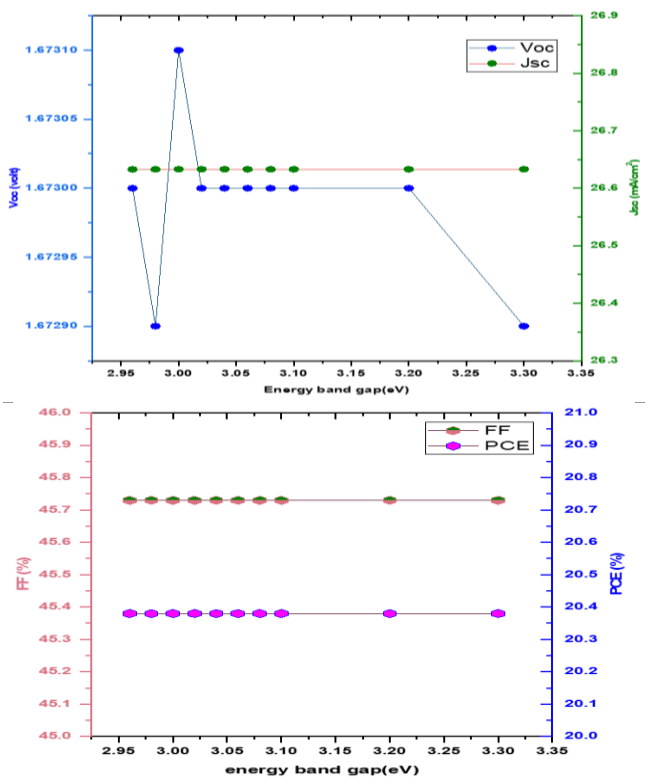


**Fig. 6:** Impact of ETL [$TiO_2$] energy band gap on $V_{oc}$(volt), $J_{sc}$(mA/cm$^2$), FF (%), and PCE (%). (a) Impact of ETL $TiO_2$ energy band gap on Voc(volt) and Jsc(mA/cm$^2$). (b) Impact of ETL $TiO_2$ energy band gap on FF (%) and PCE (%).

### 3.4 Effect of electrode layer (Ni) Thickness.

Figure [7] shows the variation of photovoltaic parameters concerning the electrode layer's thickness Ni, the work function of Nickel 5.22eV.

We observe that increasing the back electrode thickness (Ni) has a clear influence on the solar cell parameter, as shown in Figure 7, Variation layer thickness from 0.1 to 1 µm. The Voc ranges from 1.35V at 0.1µm to 3.52V at 1µm. Jsc remains mostly constant as thickness varies. The FF drops from 55.44% at 0.1µm to 22.35% at 1µm. PCE(η) increased from 18.58% at 0.1µm to 19.48% at 1µm. These results can be explained through a Schottky diode, where the metal and a semiconductor material are combined to create a diode there will be a transition in which some electrons from the metal enter the semiconductor and others from the semiconductor enter the metal. More electrons will transit from the semiconductor into the metal than in the revised way because there is a greater barrier preventing transit electrons from the metal. Which consists of two solar cells one of them perovskites and the other is Schottky diode solar cells which create tandem solar cells, yielding higher overall efficiency[32]. The optimum thickness of the back electrode of the proposed solar cell was chosen at 0.5µm.

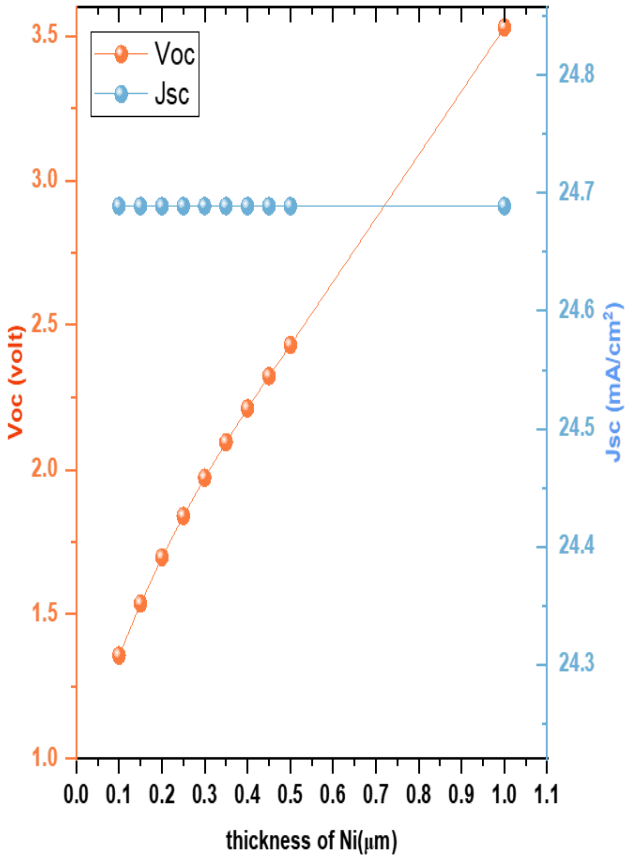

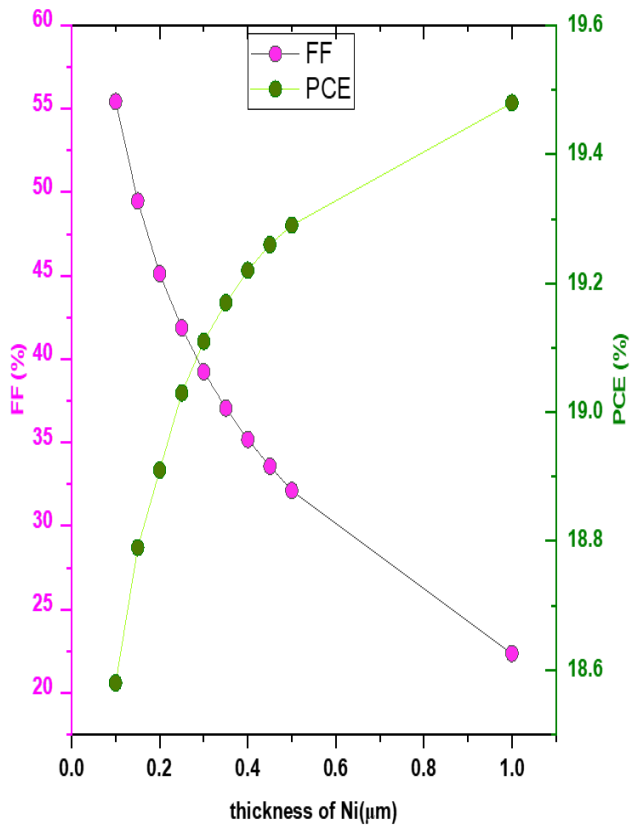


**Fig. 7:** Impact of back electrode [Ni] thick-ness on $V_{oc}$(volt), $J_{sc}$(mA/cm$^2$), FF (%), and PCE (%). (a) Impact of back electrode (Ni) thickness on Voc(volt) and Jsc(mA/cm$^2$). (b) Impact of back electrode (Ni) thickness on FF (%) and PCE (%).

### 3.5 Effect of Working Temperature on solar cell performance

The operating temperature of a solar cell device influences its performance. Higher working temperatures of photovoltage devices improve hole and electron mobilities, as well as material carrier concentrations. The temperature was changed from 253 K - to 318 K to determine its effect on solar cells and the following outcomes can be seen in Figure (8). The $V_{oc}$ increases from 1.026V at 253k to 2.019V at 318k. such results might be explained using Eq. (6), in which the reverse saturation current ($I_o$) reduces, as does the recombination probability for the charge carriers as temperature increases, And so the $V_{OC}$ grows with higher temperatures[24]. In contrast, the values of $J_{sc}$ show a small rise from 26.564 mA/cm$^2$ to 26.653 mA/cm$^2$ with rising operating temperatures, owing to the increase in the creation of electron-hole pairs[33]. The results indicate a variation in the FF value from 71.51% to 38.33% and the PCE (η) value from 19.5% to 20.63% with the temperature change. This can be explained by Eq. [4,5]. These findings demonstrate that the suggested solar cell performs well over a wide range of temperatures and with excellent efficiency.

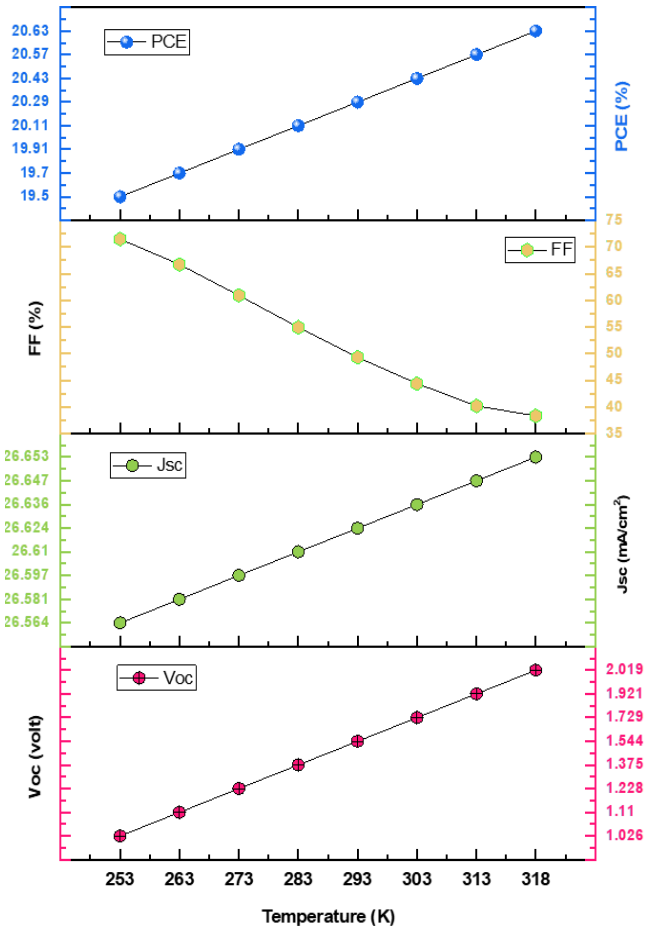


**Fig. 8:** The variation of Voc(v), Jsc(mA/cm2), FF (%), PCE (η) (%) with different temperature.

## 4 Conclusion

This work employed simulation to analyze the device structure of (FTO/TiO2/CH3NH3pbI3/CuI/Ni) while studying the band gap and thickness of the absorber layer, hole transport layer CuI, as well as the electron transport layer $TiO_2$. In addition to study electrode (Ni) thickness. Furthermore, the working temperature is adjusted between 253K and 318K by using SCAPS-1D.

Based on our modeling, we found that the ideal thickness and band gap for the active material CH3NH3pbI3 are 1µm and 1.5eV, respectively. Furthermore, the ideal values for the CuI layer at 0.1µm and 3.03 eV, and the ideal values for the $TiO_2$ layer at 0.05µm and 3eV. Finally, we obtained the ideal electrode thickness at 0.5µm. After examining the temperature variation, we discovered that the cell operates more efficiently at higher temperatures. Accordingly, the cell parameters at 318k are: $V_{oc}$=2.019v, Jsc=26.653mA/cm$^2$, FF=38.33%, PCE(η)=20.63%.

This illustrates the possibility of designing environmentally friendly beneficial, lead-based perovskite solar cells with excellent efficiency.

## Acknowledgments

We thank Dr. Marc Burgelman and his colleagues from the University of Gent, Belgium's Department of Electronics and Information Systems (ELIS), for providing the SCAPS-1D simulation software.

## Conflicts of Interest Statement

The authors certify that they have NO affiliations with or involvement in any organization or entity with any financial interest (such as honoraria; educational grants; participation in speakers' bureaus; membership, employment, consultancies, stock ownership, or other equity interest; and expert testimony or patent-licensing arrangements), or non-financial interest (such as personal or professional relationships, affiliations, knowledge or beliefs) in the subject matter or materials discussed in this manuscript.

## References

[1] A. O. M. Maka and J. M. Alabid, "Solar energy technology and its roles in sustainable development," *Clean Energy*, vol. 6, no. 3, pp. 476–483, 2022, doi: 10.1093/ce/zkac023.

[2] G. Perrakis *et al.*, "Transparent Multispectral Photonic Electrode for All-Weather Stable and Efficient Perovskite Solar Cells," *arXiv*, pp. 1–20, 2023, doi: 10.48550/arXiv.2308.03386.

[3] V. La Ferrara, A. De Maria, and G. Rametta, "Green Anisole as Antisolvent in Planar Triple-Cation Perovskite Solar Cells with Varying Cesium Concentrations," *Micromachines*, vol. 15, no. 1, 2024, doi: 10.3390/mi15010136.

[4] R. A. Afre and D. Pugliese, "Perovskite Solar Cells: A Review of the Latest Advances in Materials, Fabrication Techniques, and Stability Enhancement Strategies," *Micromachines*, vol. 15, no. 2, 2024, doi: 10.3390/mi15020192.

[5] Y. Raoui, H. Ez-Zahraouy, S. Kazim, and S. Ahmad, "Energy level engineering of charge selective contact and halide perovskite by modulating band offset: Mechanistic insights," *J. Energy Chem.*, vol. 54, pp. 822–829, 2021, doi: 10.1016/j.jechem.2020.06.030.

[6] M. G. K. Constantinos C. Stoumpos, Christos D. Malliakas, "Semiconducting Tin and Lead Iodide Perovskites with Organic Cations: Phase Transitions, High Mobilities, and Near-Infrared Photoluminescent Properties," *Inorg. Chem.*, vol. 52, no. 15, pp. 8285–9162, 2013, [Online]. Available: https://pubs.acs.org/doi/10.1021/ic401215x

[7] M. G. Ju, J. Dai, L. Ma, and X. C. Zeng, "Perovskite Chalcogenides with Optimal Bandgap and Desired Optical Absorption for Photovoltaic Devices," *Adv. Energy Mater.*, vol. 7, no. 18, pp. 1–8, 2017, doi: 10.1002/aenm.201700216.

[8] T. Ibn-Mohammed *et al.*, "Perovskite solar cells: An integrated hybrid lifecycle assessment and review in comparison with other photovoltaic technologies," *Renew. Sustain. Energy Rev.*, vol. 80, no. November 2015, pp. 1321–1344, 2017, doi: 10.1016/j.rser.2017.05.095.

[9] A. Babayigit *et al.*, "Assessing the toxicity of Pb-and Sn-based perovskite solar cells in model organism Danio rerio," *Sci. Rep.*, vol. 6, pp. 1–11, 2016, doi: 10.1038/srep18721.

[10] U. Mandadapu, "Simulation and Analysis of Lead based Perovskite Solar Cell using SCAPS-1D," *Indian J. Sci. Technol.*, vol. 10, no. 1, pp. 1–8, 2017, doi: 10.17485/ijst/2017/v11i10/110721.

[11] R. Sharif *et al.*, "A comprehensive review of the current progresses and material advances in perovskite solar cells," *Nanoscale Adv.*, vol. 5, no. 15, pp. 3803–3833, 2023, doi: 10.1039/d3na00319a.

[12] H. Liu, Z. Huang, S. Wei, L. Zheng, L. Xiao, and Q. Gong, "Nano-structured electron transporting materials for perovskite solar cells," *Nanoscale*, vol. 8, no. 12, pp. 6209–6221, 2016, doi: 10.1039/c5nr05207f.

[13] T. Mansor, "Quantum Efficiency of CdS, CdSe and TiO 2 Quantum Dot Solar Cells," University of Thi-Qar, 2017.

[14] G. Qin and A. Watanabe, "Surface Texturing of TiO 2 Film by Mist Deposition of TiO 2 Nanoparticles," *Nano-Micro Lett.*, vol. 5, no. June, pp. 129–134, 2013, [Online]. Available: http://dx.doi.org/10.5101/nml.v5i2.p129-134

[15] L. Zhu, "Development of Metal Oxide Solar Cells through Numerical Modelling," p. 85, 2012.

[16] O. Madkhali, "Structural, optical and electrical properties of copper and silver-copper iodide thin films To cite this version : HAL Id : tel-03667929 soutenance et mis à disposition de l ' ensemble de la Contact : ddoc-theses-contact@univ-lorraine.fr," pp. 9–14, 2023.

[17] A. Liu, H. Zhu, M. G. Kim, J. Kim, and Y. Y. Noh, "Engineering Copper Iodide (CuI) for Multifunctional p-Type Transparent Semiconductors and Conductors," *Adv. Sci.*, vol. 8, no. 14, pp. 1–19, 2021, doi: 10.1002/advs.202100546.

[18] C. Yang, M. Kneib, M. Lorenz, and M. Grundmann, "Room-Temperature synthesized copper iodide thin films degenerate p-Type transparent conductor with a boosted figure of merit," *Proc. Natl. Acad. Sci. U. S. A.*, vol. 113, no. 46, pp. 12929–12933, 2016, doi: 10.1073/pnas.1613643113.

[19] N. Yamada, R. Ino, and Y. Ninomiya, "Truly

Transparent p-Type γ-CuI Thin Films with High Hole Mobility," *Chemistry of Materials*, vol. 28, no. 14. pp. 4971–4981, 2016. doi: 10.1021/acs.chemmater.6b01358.

[20] S. Uthayaraj, D. G. B. C. Karunarathne, and G. R. A. Kumara, "Powder Pressed Cuprous Iodide ( CuI ) as A Hole," *Materials (Basel).*, vol. 12, no. 2037, pp. 1–9, 2019.

[21] U. Mandadapu, S. V. Vedanayakam, K. Thyagarajan, and B. J. Babu, "Optimisation of high-efficiency tin halide perovskite solar cells using SCAPS-1D," *Int. J. Simul. Process Model.*, vol. 13, no. 3, pp. 221–227, 2018, doi: 10.1504/ijspm.2018.093097.

[22] S. Kohnehpoushi, P. Nazari, and B. A. Nejand, "MoS 2 : a two-dimensional hole-transporting material for high-efficiency, low-cost perovskite solar cells," 2018.

[23] S. K. Biswas, M. K. Mim, and M. M. Ahmed, "Design and Simulation of an Environment-Friendly ZrS2/CuInS2Thin Film Solar Cell Using SCAPS 1D Software," *Hindawi Adv. Mater. Sci. Eng.*, no. 16878442, p. 10, 2023, doi: 10.1155/2023/8845555.

[24] M. Abdelfatah, A. M. El Sayed, W. Ismail, S. Ulrich, V. Sittinger, and A. El-Shaer, "SCAPS simulation of novel inorganic ZrS2/CuO heterojunction solar cells," *Sci. Rep.*, vol. 13, no. 1, pp. 1–14, 2023, doi: 10.1038/s41598-023-31553-4.

[25] S. K. Biswas, M. S. Sumon, K. Sarker, M. F. Orthe, and M. M. Ahmed, "A Numerical Approach to Analysis of an Environment-Friendly Sn-Based Perovskite Solar Cell with SnO2Buffer Layer Using SCAPS-1D," *Adv. Mater. Sci. Eng.*, vol. 2023, 2023, doi: 10.1155/2023/4154962.

[26] H. J. Park, H. Son, and B. S. Jeong, "SCAPS-1D Simulation for Device Optimization to Improve Efficiency in Lead-Free CsSnI3 Perovskite Solar Cells," *Inorganics*, vol. 12, no. 4, 2024, doi: 10.3390/inorganics12040123.

[27] R. Ranjan *et al.*, "SCAPS study on the effect of various hole transport layer on highly efficient 31.86% eco-friendly CZTS based solar cell," *Sci. Rep.*, vol. 13, no. 1, pp. 1–16, 2023, doi: 10.1038/s41598-023-44845-6.

[28] V. Jha, S. Dasgupta, and A. Ganguly, "Study of PbS Nanomaterial Sensitized ZnO based Solar Cell using SCAPS-1D Simulator," *2023 Int. Symp. Devices, Circuits Syst. ISDCS 2023 - Conf. Proc.*, no. May 2023, pp. 2–5, 2023, doi: 10.1109/ISDCS58735.2023.10153556.

[29] M. S. Islam *et al.*, "Defect study and modeling of SnX3-based perovskite solar cells with SCAPS-1D," *Nanomaterials*, vol. 11, no. 5, 2021, doi: 10.3390/nano11051218.

[30] O. A. Muhammed, D. Eli, P. H. Boduku, J. Tasiu, M. S. Ahmad, and N. Usman, "Modeling and simulation of lead-free perovskite solar cell using scaps-1D," *East Eur. J. Phys.*, vol. 2021, no. 2, pp. 146–154, 2021, doi: 10.26565/2312-4334-2021-2-12.

[31] N. S. N. M. Alias, F. Arith, A. N. Mustafa, M. M. Ismail, N. F. Azmi, and M. S. Saidon, "Impact of Al on ZnO Electron Transport Layer in Perovskite Solar Cells," *J. Eng. Technol. Sci.*, vol. 54, no. 4, 2022, doi: 10.5614/j.eng.technol.sci.2022.54.4.9.

[32] "The Metal - Semiconductor Junction. Schottky Diode." [Online]. Available: https://in.ncu.edu.tw/ncume_ee/SchottkyDiode.htm

[33] M. F. Wahid, U. Das, B. K. Paul, S. Paul, M. N. Howlader, and M. S. Rahman, "Numerical Simulation for Enhancing Performance of MoS2 Hetero-Junction Solar Cell Employing Cu2O as Hole Transport Layer," *Mater. Sci. Appl.*, vol. 14, no. 09, pp. 458–472, 2023, doi: 10.4236/msa.2023.149030.